

Experimental Investigation of the Cooperative Jahn-Teller Effect in TmCd[†]

B. Lüthi and M. E. Mullen

Physics Department, Rutgers University, New Brunswick, New Jersey 08903

K. Andres, E. Bucher, and J. P. Maita

Bell Telephone Laboratories, Murray Hill, New Jersey 07974

(Received 26 March 1973)

TmCd has the CsCl structure and shows a Jahn-Teller distortion to a tetragonal structure at $T_a = 3.16$ K. Specific-heat, electrical-resistance, and elastic measurements show that the ground state of the Tm^{3+} ion is a nonmagnetic Γ_3 doublet. The next-higher excited level is at approximately 20 K. We do not find evidence for magnetic ordering down to 40 mK. The susceptibility and high-field magnetization can be interpreted with these crystal-field levels without taking exchange into account. The elastic c_{44} mode shows a small anomaly of 0.9% at T_a , whereas the $c_{11}-c_{12}$ mode shows strong softening below 100 K of 33% down to T_a . We can interpret the temperature dependence of this mode quantitatively. High magnetic fields have a profound influence on these elastic constants and electrical resistivity. We find an apparent increase of T_a for magnetic fields applied in the [100] direction and somewhat smaller effects for other directions. We explain this effect tentatively by showing that the first-order transition is shifted in high fields to higher temperatures and that the discontinuity in the order parameter diminishes continuously with increasing field.

I. INTRODUCTION

Crystal structure changes originating from the Jahn-Teller effect have been known for some time for transition-metal-ion compounds¹ (spinel and perovskite). More recently it was also found that rare-earth ions with degenerate or nearly degenerate orbital ground states exhibit such effects in vanadates, arsenates, and phosphates² (e.g., DyVO_4 , TbVO_4 , TmAsO_4 , TbPO_4). In these compounds the structural change is from tetragonal to orthorhombic. In addition, some rare-earth pnictides, with a rocksalt structure, show structural changes to tetragonal or trigonal symmetries.³ In this case the structural transition is accompanied by a magnetic transition.⁴ In this paper we show that TmCd, which crystallizes in the cubic CsCl structure, is another example of a compound which exhibits a Jahn-Teller distortion.

There are various experimental tools to investigate and characterize such transitions. One of the most useful and direct ones is to measure the elastic constant, which is related to the elastic symmetry strain describing this transition. What one observes generally is a softening of this elastic constant as one approaches the transition temperature T_a from the high-temperature phase. Such experiments have been carried out in a number of systems: UO_2 ,⁵ NiCr_2O_4 ,⁶ CsCuCl_3 ,⁷ DyVO_4 ,^{8,9} TbVO_4 ,⁹ TmAsO_4 ,¹⁰ DySb .^{11,12} What one usually gets from such experiments is the relative importance of the strain coupling to the electronic states, compared to other types of coupling (via optical phonon, direct quadrupole interaction, etc.)

In this paper we describe experiments performed

on TmCd. This substance has the CsCl structure and undergoes a structural transition at 3.16 K to a tetragonal phase. There is no sign of a magnetic phase transition down to 0.04 K. This material is unique in that it has, apart from the Γ_3 ground state, low-lying higher-crystal-field levels Γ_5 , Γ_2 of the ground-state multiplet 3H_6 of the Tm^{3+} ion. These crystal-field levels affect the electrical resistance, the magnetization, the specific heat, and the elastic constants considerably in the temperature region $T < 100$ K. We are able to account for these effects in a quantitative manner. In addition, we observe rather spectacular effects for the electrical resistance and the symmetry elastic constant $c_{11} - c_{12}$ by application of high magnetic fields. A compilation of physical constants, mainly deduced from this study, is given in Table I.

In Secs. II–IV we describe experimental details, the theory necessary to describe our results and finally we discuss and compare our experimental results with the theoretical predictions.

II. EXPERIMENT

TmCd was obtained by direct fusion of the components in sealed Ta crucibles. The fine-grained material was transferred into a Bridgman crucible which was subsequently sealed by an electron-beam method. The crucible was heated in a cylindrical furnace of Ta, carrying a temperature gradient of about 10 °C/cm. The crucible was lowered at a rate of ~1 in./h, leading to directional solidification (Bridgman method). The resulting piece consisted of crystallites approximately 3 mm in size.

We cut [110] and [100] oriented specimens, which consisted of thin disks for the magnetic and electri-

cal measurements and of 2-mm-thick cylinders, polished on both end faces, for the elastic measurements.

Susceptibility measurements at 15 kOe were made with a pendulum magnetometer¹⁴ and at higher and lower fields with a flux-gate magnetometer. The latter method consists on leaving the sample inside a superconducting magnet and transforming its magnetic flux with a superconducting transformer to a shielded coil outside the magnet where it can be monitored with a flux-gate-magnetometer probe.

The electrical-resistance measurements were made with a low-frequency ac current using the standard four-lead technique. Specific-heat measurements above 2 K were made in a heat-pulse calorimeter described elsewhere.¹⁵ Hyperfine specific-heat measurements below 0.2 K were carried out in an adiabatic-demagnetization cryostat.

The elastic constants were measured with a phase-comparison method,¹⁶ capable of detecting changes in one part in 10^6 in our case. We used various ultrasonic bonds; Dow Corning 200 fluids of various viscosities or a thin indium film proved best. No thermal-expansion correction was made for the elastic constants, as they usually are negligible.

Superconducting magnets up to 60 kOe were used for the high fields. The temperature was measured with calibrated Ge resistors and thermocouples.

III. THEORY

We discuss here the crystal-field levels for the Tm^{3+} ion, the magnetic field dependence of these levels, the magnetic-susceptibility calculation, the cooperative Jahn-Teller effect and the effect of the higher-crystal-field levels on the elastic constants.

A. Crystal-Field Levels

The Tm^{3+} ion has a free-ion ground state 3H_6 . The $J=6$ ground-state multiplet splits in a cubic field into Γ_1 , Γ_2 , Γ_3 , Γ_4 , and two Γ_5 states. The Tm^{3+} ion has cubic coordination with eight equidistant anion charges in the CsCl structure. With the point-charge calculation of Lea, Leask, and Wolf¹⁷ this leads to negative values for B_4 and B_6 , the parameters of the fourth- and sixth-order crystal-field terms. This in turn leads to positive x and negative W , two new parameters, measuring the ratio of B_4 and B_6 and the scaling of the crystal-field energy levels.¹⁷ One finds¹⁷ for $0.8 < x \leq 1$, that Γ_3 is the ground state with a Γ_5 and a Γ_2 level lying closest and a rather large gap for the remaining levels. From specific-heat and elastic-constant measurements, discussed below, there is evidence that Γ_3 is indeed the ground-state level. Electrical-resistance measurements discussed below show that the first excited state has an energy

TABLE I. Physical constants.

Thermal data:	density = 9.47 g/cm ³ , elastic constants at 300 K in (10^{11} erg/cm ²): $c_{11} = 7.74$, $c_{12} = 4.59$, $c_{44} = 4.38$, elastic Debye temperature $\Theta_D = 196$ K, electric resistance ratio $\rho_{300}/\rho_4 = 40$
Electronic data:	for $\text{Tm}^{3+} (4f^{12}) ^3H_6$, $p = g [J(J+1)]^{1/2} = 7.78$ (free ion $p = 7.57$), ground state Γ_3 , next higher level Γ_5 at 20 K
Structural data:	transition temperature $T_a = 3.16$ K, ratio of Jahn-Teller strain coupling to other kinds of coupling ≈ 0.3 , spontaneous strain for $T = 0$: $\langle \epsilon \rangle \approx 10^{-3}$, lattice constant ^a $a = 3.665$ Å

^aReference 13.

of ≈ 20 K. We therefore find the following level diagram, with the energies given in parentheses: Γ_3 (0 K), Γ_5 (20 K), Γ_2 (80 K), and all other levels at 300 K and higher in energy. These estimates are approximately valid for the range of x quoted above. Since we discuss mainly low-temperature properties and since we relied on point-charge calculations¹⁷ in making these estimates, we consider in our further calculations only these three lowest crystal-field levels.

B. Susceptibility and Magnetization

In order to discuss our susceptibility and high-field magnetization experiments, as well as our field-dependent elastic constants and electrical-resistance results, we need to know the magnetic field dependence of the Γ_3 , Γ_5 , and Γ_2 levels. In most cases we applied the magnetic field in a [100] or a [110] direction. We give results for a [100] direction. With first-order perturbation theory, using the tabulated wave functions¹⁷ $|\Gamma_j^i\rangle$ one has to calculate matrix elements of the form $\langle \Gamma_j^i | \mathcal{H}_Z | \Gamma_j^i \rangle$ where the Zeeman term $\mathcal{H}_Z = -g\mu_B H_x J_z$. Here g is the Landé g factor ($\frac{7}{6}$ for a 3H_6 state), μ_B the Bohr magneton, and J_z the component of the angular momentum operator along a cubic axis. The secular equation for the energy reads

$$|E_0(\Gamma_j^i) - E + \langle \Gamma_j^i | \mathcal{H}_Z | \Gamma_j^i \rangle| = 0 \quad (1)$$

where $E_0(\Gamma_j^i)$ is the energy tabulated above (see Table I). The 6×6 determinant of Eq. (1) was solved using a computer for fields up to 60 kOe and the results are shown in Fig. 1.

From these energies one can calculate the magnetization and susceptibility χ :

$$M = kT \frac{\partial}{\partial H} \ln \sum_i e^{-\beta E_i}, \quad (2)$$

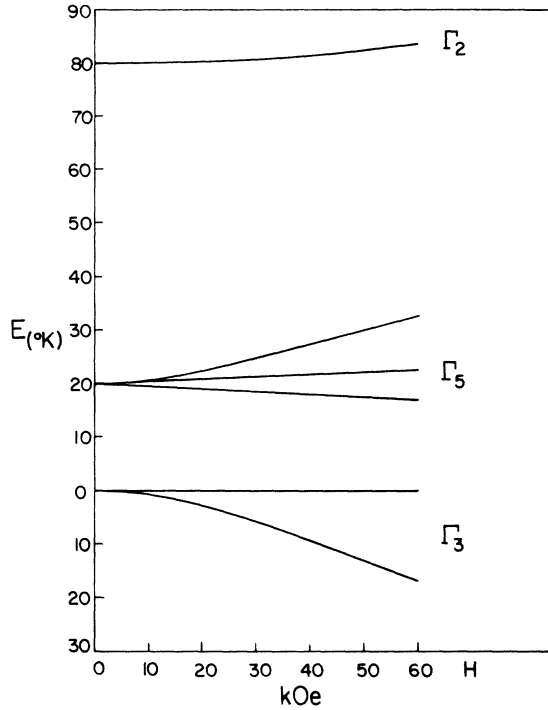


FIG. 1. Crystal-field levels as a function of a [100] magnetic field, calculated using Eq. (1).

$$\chi = \frac{\partial M}{\partial H} = kT \frac{\partial^2}{\partial H^2} \ln \sum_i e^{-\beta E_i}. \quad (3)$$

The low-field susceptibility for a cubic material is isotropic, e. g., independent of magnetic field direction. The magnetization formula above has dimensions ($^{\circ}\text{K}/\text{ion G}$). In order to change it to the usual one (emu/g) one has to multiply by 2.96×10^5 (with the measured density from Table I). The calculated susceptibility and magnetization values are shown and discussed with the experiment below (see Figs. 5 and 7).

C. Cooperative Jahn-Teller Effect and Elastic-Constant Calculation

In recent years several theories of the cooperative Jahn-Teller (J-T) effect have been developed for transition-metal compounds having the spinel structure¹⁸ and for rare-earth compounds, especially the vanadates.^{2,19} Particular emphasis was given in these theories to the softening of a particular elastic constant associated with the symmetry strain. An important interaction term for the J-T effect is the coupling of the macroscopic symmetry strain to the electronic states, occurring for example via strain modulation of the crystal field. For TmCd the soft elastic constant is $c_{11} - c_{12}$ which belongs to a two-dimensional representation Γ_3 with the two symmetry strains $\epsilon_2 = \sqrt{\frac{1}{2}}(\epsilon_{xx} - \epsilon_{yy})$ and

$\epsilon_3 = \sqrt{\frac{1}{6}}(2\epsilon_{zz} - \epsilon_{xx} - \epsilon_{yy})$ which leads to a cubic-tetragonal transition. The interaction Hamiltonian reads:

$$\mathcal{H}_1 = -g_0 \left(\frac{c_0}{N} \right)^{1/2} \sum_i (\epsilon_2 O_{2,i}^2 + \epsilon_3 O_{2,i}^0), \quad (4)$$

where g_0 is the coupling constant, $c_0 = c_{11} - c_{12}$, N is the number of Jahn-Teller ions, and $O_2^2 = \sqrt{3}(J_x^2 - J_y^2)$, $O_2^0 = 3J_z^2 - J(J+1)$ are the Stevens operators describing the electronic states.²⁰ If one acts with (4) on the crystal-field states $|\Gamma_j^i\rangle$ one gets a splitting of the levels in the following form: Since in the cubic phase c_0 is degenerate, we set $\epsilon_2 = 0$ and denote $\epsilon_3 = \epsilon$. The secular determinant gives

$$\begin{aligned} E(\Gamma_3^{1,2}) &= \pm g_0 (c_0/N)^{1/2} \epsilon = 35.9989, \\ E(\Gamma_5^1) &= 20 - g_0 (c_0/N)^{1/2} \epsilon = 64.2102, \\ E(\Gamma_5^{2,3}) &= 20 + g_0 (c_0/N)^{1/2} \epsilon = 32.0994, \quad E(\Gamma_2) = 80. \end{aligned} \quad (5)$$

Here the numerical factors are the values for the matrix elements $\langle \Gamma_j^{i'} | O_2^0 | \Gamma_j^i \rangle$. It is this linear strain dependence of the energy levels which leads, with the positive elastic energy, quadratic in the strain, to a lower symmetry structure with a spontaneous strain $\langle \epsilon \rangle \neq 0$ below a transition temperature T_c . The cooperative effect arises, because (4) leads to an effective two-ion coupling of infinite range $-(g_0^2/2N) \sum_{i,j} (O_{2,i}^0 O_{2,j}^0)$ if one transforms (4) with a transformation,^{2,18} $\epsilon' = \epsilon - [g_0/(c_0 N)^{1/2}] \sum_i O_{2,i}^0$. To make the theory more complete one usually adds other two-ion terms to (4), which arise from other quadrupole-quadrupole interactions^{2,18}:

$$\mathcal{H}_2 = -g_i \left(\frac{A}{N} \right)^{1/2} \sum_j (\langle O_2^2 \rangle O_{2,j}^2 + \langle O_2^0 \rangle O_{2,j}^0), \quad (6)$$

where g_i is the coupling constant and the term is written down in molecular-field approximation.

The elastic constants can be calculated by calculating the strain dependence of the energy levels with (4) and (6) and as shown in (5), constructing the free energy and taking the second derivative respect to ϵ : $c_{11} - c_{12} = \partial^2 F / \partial \epsilon^2$. Note that $\partial F / \partial \epsilon = 0$ and $\partial F / \partial \langle O_2^0 \rangle = 0$ give a linear relation between the spontaneous strain $\langle \epsilon \rangle$ and the order parameter $\langle O_2^0 \rangle$ and the temperature dependence of the latter. Such a calculation for the lowest-crystal-field state has been performed before^{2,6,18} and the result for the high-temperature phase $T > T_c$ can be put into the following simple form:

$$\frac{c_{11} - c_{12}}{c_0} = \frac{T - T_c}{T - \Theta}, \quad (7)$$

where $kT_c = \frac{1}{2}(g_0^2 + g_i^2)$ is the transition temperature if the transition were of second order and $k\Theta = \frac{1}{2}g_i^2$ is the transition temperature if no macroscopic strains are allowed. $c_0 = c_{11} - c_{12}$ is the elastic constant in the absence of a cooperative J-T effect. Equation (7) and slight variations from it have been

successfully tested for various systems.⁶⁻⁹

In the case of TmCd, Eq. (7) neglects some important points: First, the cubic-tetragonal transition with the two-dimensional symmetry strains ϵ_2, ϵ_3 allows higher-order (cubic) Jahn-Teller terms and cubic anharmonic terms, which change the transition from second order to first order.¹⁸ If we confine ourselves to the high-temperature phase, these terms do not contribute to the elastic constants and Eq. (7) still holds. But we will make use of this fact when we discuss high-magnetic-field effects. Second, the higher-crystal-field levels lie in a region where we want to make a quantitative comparison with theory. Therefore one has to take them into account in a proper calculation of the elastic constants. There are three ways in which excited crystal-field levels have an effect on the elastic constants: Through a depopulation effect due to Boltzmann factors, through the energy splitting due to the J-T effect as calculated in Eq. (5) and through an effect due to the noncommutativity²¹ of the crystal-field operators O_4, O_6 and the Jahn-Teller operator O_2^0 . Such effects had to be taken into account previously for DySb.¹² We only quote the final formula, since the derivation is lengthy. Basically the two constants T_c and θ in Eq. (7) are replaced by temperature averages of the O_2^0 operator²¹:

$$c_{11} - c_{12} = c_0 \frac{T - (g_0'^2 + g_1'^2) \chi(T)}{T - g_1'^2 \chi(T)}, \quad (8)$$

$$\chi(T) = \frac{1}{\sum_m e^{-\beta E_m}} \left(\sum_m e^{-\beta E_m} \left| O_{2,mm}^0 \right|^2 \right)$$

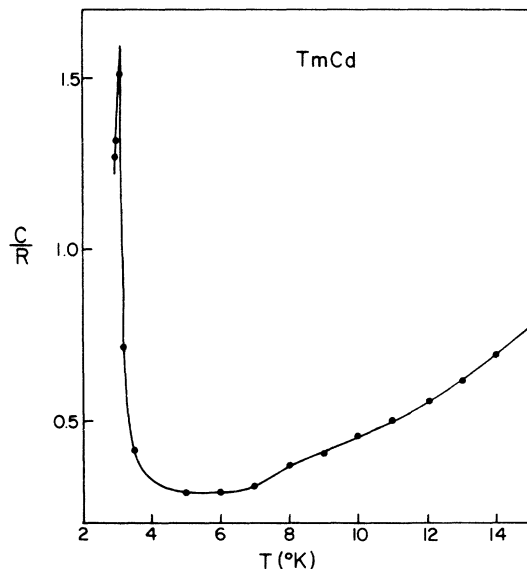


FIG. 2. Specific heat C/R as a function of temperature for TmCd.

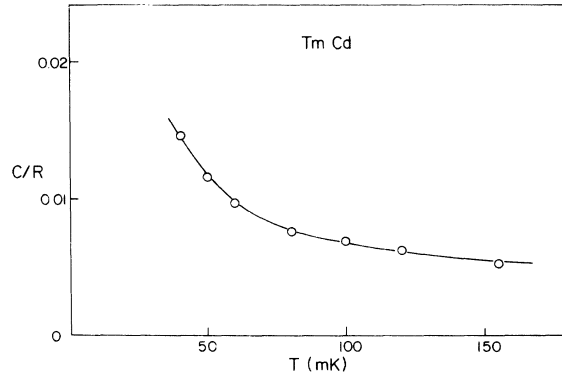


FIG. 3. Hyperfine specific heat C/R as a function of temperature in the mK region for TmCd.

$$-2 \sum_{n>m} \frac{e^{-\beta E_m} - e^{-\beta E_n}}{\beta(E_m - E_n)} \left| O_{2,nn}^0 \right|^2 \right).$$

Depending on the temperature, the term with the nondiagonal matrix elements makes a contribution between 5% and 25% to the total $\chi(T)$. Application of this formula to TmCd will be given in Sec. IV, Fig. 10.

IV. RESULTS AND DISCUSSION

We present here our results on specific heat, electrical resistivity, magnetization, and elastic constants and discuss them in the light of the theories outlined above. A short account of these results was given elsewhere.²²

A. Specific Heat

Specific-heat measurements are shown in Fig. 2. Above 4 K there is evidence of a broad Schottky-type specific-heat anomaly due to the excited crystal-field levels. If the ground state of Tm^{3+} were a singlet, this specific-heat contribution should decay exponentially towards 0 K. Instead we observe a large and sharp maximum in the specific heat at 3.1 K. Since there is no magnetic order occurring at this temperature (see below), this anomaly must be due to the cooperative splitting of a nonmagnetic Γ_3 doublet. This assumption is confirmed by hyperfine specific-heat measurements below 0.15 K (Fig. 3). Even at 40 mK the nuclear-specific-heat contribution is very small ($C/R \approx 1.5 \times 10^{-2}$), indicating that the Tm^{3+} is indeed in a nonmagnetic ground state.

B. Electrical Resistivity in the Absence of a Magnetic Field

In Fig. 4 we show the electrical resistivity as a function of temperature for a polycrystalline sample, with single-crystal samples exhibiting the same features. Apart from a linear temperature dependence, one notices two kinks in the curve, one at ≈ 3 K due to the Jahn-Teller transition (in

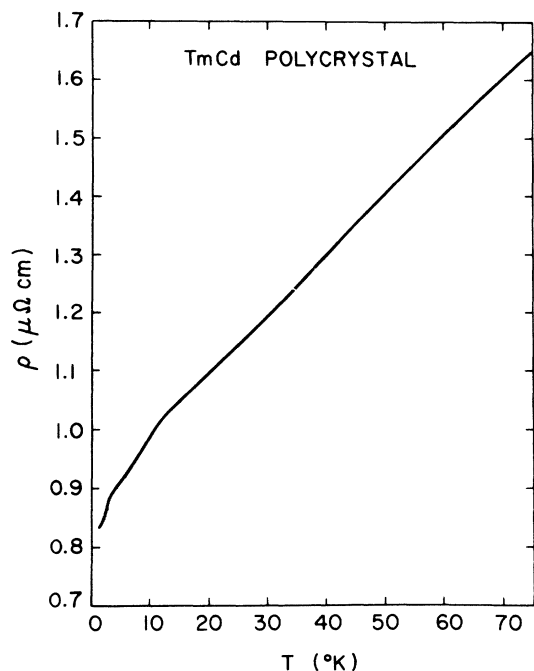


FIG. 4. Electrical resistivity ρ of a polycrystalline TmCd sample as a function of temperature.

single-crystal samples it occurs at 3.16 K) and one at 11.5 K which we interpret as due to a higher-lying crystal-field level about 20 K above the ground state. This interpretation was deduced from analogous cases, where the crystal-field levels are known from measurements by neutron scattering.²³ In PrSb with an excited state Γ_4 at 73 K one finds a kink at 40 K and for PrCu₂ with a singlet state at 13 K one finds a kink at 7 K.²⁴ In our case, a kink at 11.5 K implies an energy of about 20 K for the Γ_5 level. The next Γ_2 level lies then at about 80 K.¹⁷ Such an energy-level scheme we have used in Sec. III for our calculation. It should be pointed out that to the best of our knowledge no theory exists so far for the electrical resistivity due to electron scattering at crystal-field levels.

C. Magnetic Susceptibility

In Fig. 5 we show the inverse magnetization as a function of temperature for a field of 14.24 kOe. From Fig. 1 and Ref. 25 we notice that with such a field we still measure essentially isotropic low-field behavior. The experimental points show a typical Van Vleck susceptibility behavior. The full line is $1/M$ calculated using Eq. (2) and the crystal-field levels of Fig. 1, but neglecting exchange. In other Tm compounds, TmSb, TmAs, one also could interpret the experimental results using crystal-field effects only.²⁶ The reason for this is presumably the fact that for the Tm³⁺ ground state 3H_6 , $L = 5$ is much larger than $S = 1$. The agreement be-

tween theory and experiment in Fig. 5 is quite satisfactory. The disagreement towards the high-temperature end is due to the chosen crystal-field-level scheme, where we have neglected higher-lying states. Indeed if we calculate at 300 K the effective number of Bohr magnetons from our experimental data, we get a value $p \approx g [J(J+1)]^{1/2} = 7.78$ compared to the free-ion value of 7.57. This indicates that we are not yet in the high-temperature region, which is in agreement with our estimated energy levels (Sec. III). The difference between the measured p and the free-ion value could also be due to Cd deficiencies in our sample.

In the low-temperature region a small anomaly is indicated in the theoretical curve at 2 K. This is due to the fact that our ground state is not a singlet but a doublet. For a temperature corresponding to the splitting in a 14-kOe field a depopulation of the upper level of the doublet occurs. No clear evidence for such an anomaly was found experimentally. It should be mentioned that in the magnetic calculations the effect of the cooperative J-T effect was neglected. Indeed there is only a very minute effect of this structural transition on the magnetic properties and only at very low fields as shown in Fig. 6, where one notices a small kink in the magnetization curve for 1 kOe at 3.16 K. This kink has completely disappeared for a field of 50 kOe. The converse, however, the effect of a magnetic field on the structural transition is very pronounced as we shall see in Sec. IV F.

D. High-Field Magnetization

Figure 7 shows high-field magnetization curves at 4.2 K for H in the [110] direction and a point for H in the [100] direction at 50 kOe. These results indicate that the [100] direction is the easy direction and [111] probably the hard direction of magnetization. In Fig. 7 we also show a calculated magnetization curve for the [100] direction. This

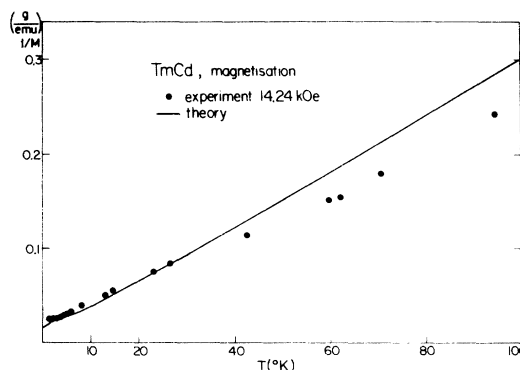


FIG. 5. Inverse magnetization $1/M$ as a function of temperature in a field of 14.24 kOe. Full line is calculated $1/M$ using energy levels of Fig. 1 and Eq. (2).

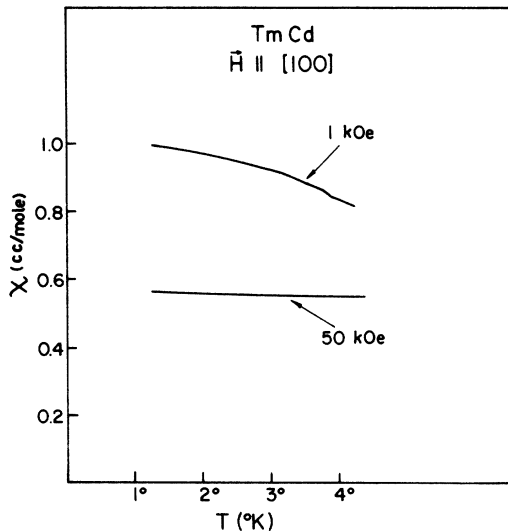


FIG. 6. Magnetization curves for 1 and 50 kOe as a function of temperature, indicating the effect of the structural transition on magnetization.

calculation was again made using Eq. (2), the energy levels of Fig. 1 and neglecting any exchange. The salient features of the experimental results are clearly reproduced: A linear field dependence up to 20 kOe, a trend towards saturation, but with

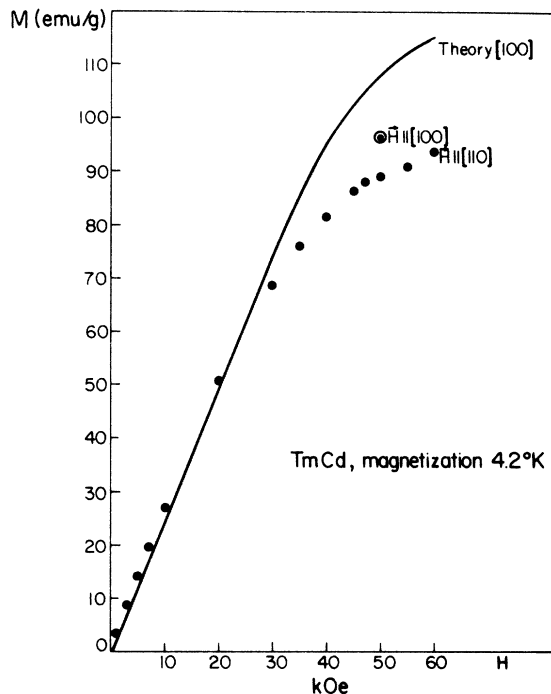


FIG. 7. High-field magnetization M vs magnetic field for [110] direction, with one point for [100] direction. Full line is calculated magnetization using Eq. (2), $T = 4.2$ K.

saturation not reached at 60 kOe. The calculated value is about 10% too high at the highest fields.

E. Elastic Constants in the Absence of a Magnetic Field

An over-all view of the elastic constants $c_{11} - c_{12}$ and c_{44} is given in Fig. 8. Whereas c_{44} shows only a small anomaly close to the Jahn-Teller transition temperature $T_a = 3.16$ K, one notices considerable softening of the $c_{11} - c_{12}$ mode for temperatures below 100 K and especially below 10 K till 3.26 K where we lose the echo due to very strong attenuation.

An expanded view of the c_{44} mode is given in Fig. 9. The small but pronounced dip at 3.16 K serves as an accurate determination of the transition temperature T_a . It agrees very well with corresponding measurements from electrical resistivity, specific heat, and susceptibility. One observes a total softening of 0.45% in velocity change or 0.9% in c_{44} . This value is very close to the one observed in DySb.^{11,12} In that material a small trigonal deformation is also observed.⁴ It is not clear at the moment whether this implies a similar small trigonal distortion in the case of TmCd.

Figure 10 shows a blown-up version of the $c_{11} - c_{12}$ mode at lower temperatures, where one can clearly see the very strong softening below 10 K. The over-all softening of this mode is 33% down to 3.26 K. At the transition temperature $T_a = 3.16$ K

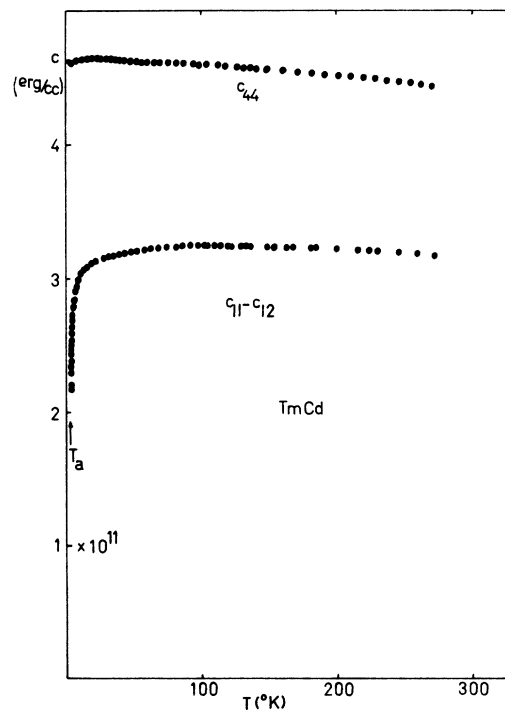


FIG. 8. Elastic constants c_{44} and $c_{11} - c_{12}$ as a function of temperature, frequency 10 MHz.

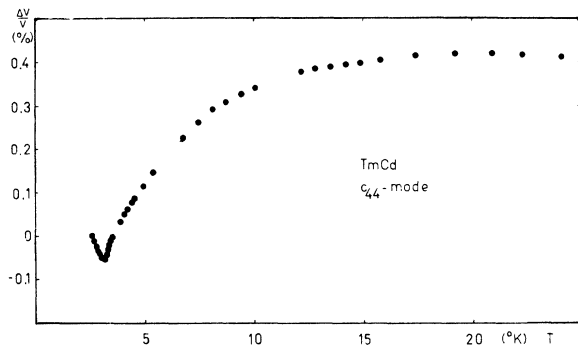


FIG. 9. Expanded plot for c_{44} mode (relative velocity change) vs temperature.

this mode is by no means completely soft, indicating a first-order transition.^{6,7} Inspection of formulas (7) or (8) indicates that this steep fall of $c_{11} - c_{12}$ below 10 K implies a rather large value of g_i compared to g_0 , i. e., considerable quadrupole-quadrupole interaction of different nature than via macroscopic strain. In trying to fit a theoretical curve to our experiments we did not get a satisfactory fit using Eq. (7) with adjustable parameters T_c, Θ . This means that the influence of the crystal-field levels Γ_5, Γ_2 is noticeable. The full line drawn in Fig. 10 is a fit using Eq. (8) and the crystal-field levels discussed in Sec. IIIA. The following parameters were used: $c_{11}^0 - c_{12}^0 = 3.26 \times 10^{11}$ erg/cm³ (assumed temperature independent for $T < 50$ K; see Fig. 8), $g_0'^2 + g_i'^2 = 1.68 \times 10^{-3}$, $g_i'^2 = 1.34 \times 10^{-3}$ which gives for $T = 0$ a $T_c = 2.2$ K, $\Theta = 1.7$ K. Such a value for T_c is reasonable since one expects for a first-order transition $T_c < T_a$. The large value of $g_i'^2$ or Θ indicates, as already mentioned, a strong Jahn-Teller coupling not originating in the coupling to the macroscopic strain to the Tm^{3+} ions. The over-all agreement between theory and experiment shown in Fig. 10 is excellent.

As mentioned above, the ultrasonic attenuation increases very strongly in the temperature region below 10 K. For 10 MHz the attenuation increases to 200 dB/cm at 3.26 K. This effect is much larger than what one usually observes at various other phase transitions.²⁷ No theory has been developed so far for the attenuation in this case, but it is clear that interesting features about the dynamics of such a phase transition could be obtained.

F. Magnetic Field Dependence of Elastic Constants and Electrical Resistivity.

Finally we give some intriguing experimental results on the effect of a magnetic field on physical quantities, such as the soft elastic constant $c_{11} - c_{12}$ and the electrical resistance. The interplay between a Zeeman term, as used in Eq. (1) for the magnetic properties and a Jahn-Teller term, as

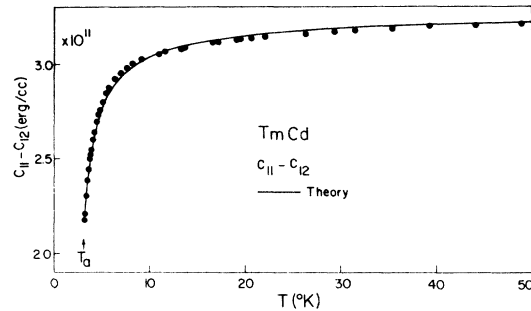


FIG. 10. Comparison between experiment and theory for the $c_{11} - c_{12}$ elastic constant. Full line is theoretical fit using Eq. (8) and parameters given in text.

used in Eqs. (4) and (6) for the structural aspects, should give interesting effects.

Previously, in other rare-earth compounds (vanadates and arsenates), one has observed a magnetic field control of the distortion direction²⁸ (magnetic switching), a washing out of the sharp transition,²⁹ similar to a ferromagnet in a magnetic field, and finally, a prevention of the distortion by application of a field in certain crystallographic directions.³⁰

We start by showing the effect of a field on the soft mode $c_{11} - c_{12}$. In Fig. 11 we show the velocity change for various field directions at 4.2 K. One notices a large increase of 6% for a [100] field of 15 kOe, but almost no change for a [111] field and a decrease of 0.5% for a [011] field up to 8 kOe after which the ultrasonic-echo pattern disappeared. In this set of experiments the field was rotated in a $\langle 110 \rangle$ plane perpendicular to the propagation di-

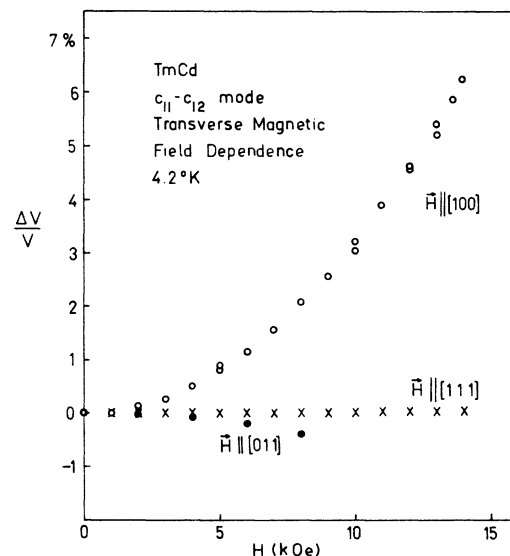


FIG. 11. Magnetic field dependence of $c_{11} - c_{12}$ mode for various magnetic field directions at $T = 4.2$ K. The field is perpendicular to the propagation direction.

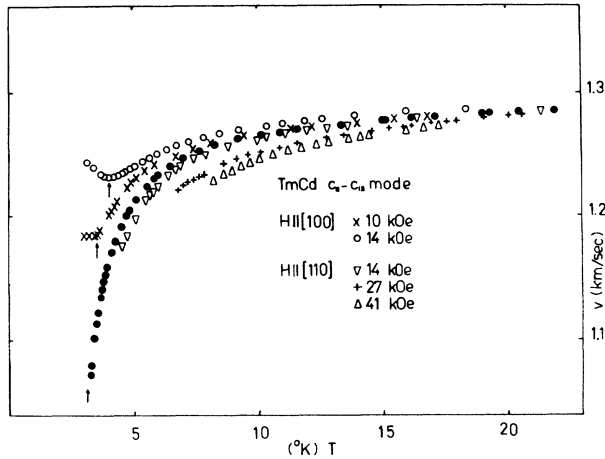


FIG. 12. Temperature and magnetic field dependence of $c_{11} - c_{12}$ mode $v = [(c_{11} - c_{12})/2\rho]^{1/2}$ for two field directions [100] and [110]. Arrows indicate T_a^x .

rection.

A clearer picture is obtained if one considers isochoamps instead of isotherms. In Fig. 12 we show the zero-field result for $c_{11} - c_{12}$ together with magnetic field results. For [100] fields the elastic constants lie above the $H = 0$ one, whereas for the [110] fields the elastic constants lie below

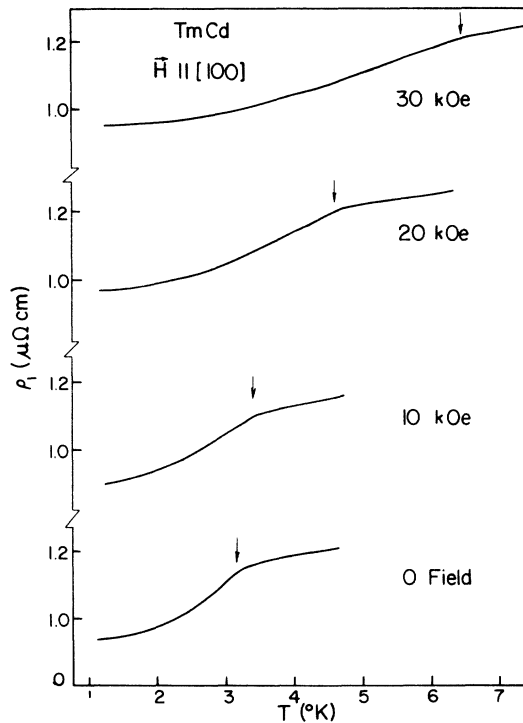


FIG. 13. Temperature and magnetic field dependence of electrical resistivity for [100] magnetic field. Arrows indicate T_a^x .

the zero-field one. Again for the [110] direction the echo pattern deteriorates due to strong attenuation, before one reaches the transition temperature. The larger the applied field, the larger the temperature where we lost the echoes. For the [100] direction one notices an anomaly in the form of a more or less abrupt change in the elastic constant. It looks as if the transition temperature T_a were enhanced in the presence of a magnetic field. The arrows indicate the temperature where the change occurs or where there is a minimum in the $c_{11} - c_{12}$ mode. We do not offer here an explanation of the detailed field dependence of $c_{11} - c_{12}$ mode and its attenuation in the presence of a magnetic field. Rather we try to understand what happens to the order parameter in the presence of a magnetic field.

To do this, we show corresponding results for the electrical resistivity in magnetic fields in Fig. 13. One sees that for increasing fields in the [100] direction the kink occurring at T_a for $H = 0$, moves to higher T . At the same time the kink becomes less and less pronounced, till after 50 kOe one no longer can notice it.

The temperature T_a^x at which this kink occurs, is plotted as a function of field in Fig. 14 for three field directions [100], [110], [111]. The two points from the [100] elastic-constant minimum of Fig. 11 are also included. One notices a rapid increase for T_a^x for $\vec{H} || [100]$, almost no change for small $\vec{H} || [111]$ in agreement with results of Fig. 11 and first a slight negative change of T_a^x for the [110] direction followed by a positive increase at higher fields.

We propose the following simple explanation for these phenomena: The first-order phase transition persists in the presence of a field and shifts to higher temperatures. The jump in the order parameter decreases with increasing field and is washed out completely for high-enough fields. The

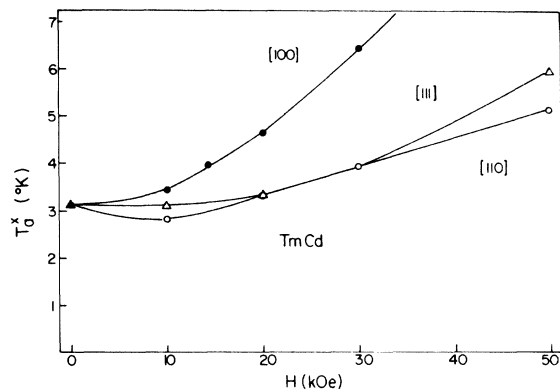


FIG. 14. T_a^x vs magnetic field for various field directions. Experimental points taken from Figs. 12 and 13.

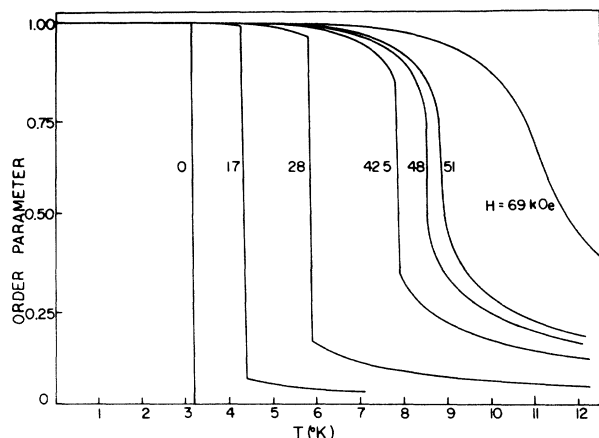


FIG. 15. Temperature and magnetic field dependence of normalized order parameter. Parameters used are $T_c = 0.75$ K, $\delta = 0$, $T'_c = T_c c_0 / 2\alpha = 0.9$ K. The numbers on each curve indicate the magnetic field in kOe.

kinks in the electrical resistance and the $c_{11} - c_{12}$ mode occur where the order parameter shows its discontinuity.

We show this with a simple model calculation. Equation (4) is not sufficient for a first-order transition. One has to include terms of higher order as mentioned before¹⁸: $\mathcal{H}_a = \delta(\epsilon_3^3 - 3\epsilon_2^2 \epsilon_3)$ and $\mathcal{H}^1 = -\alpha \sum_i [\epsilon_3^2 - \epsilon_2^2] O_{2,i}^0 - 2\epsilon_2 \epsilon_3 O_{2,i}^1$. Together with the Zeeman term one can calculate the energies $E(\Gamma_j^i)$. For illustration purposes we set $\delta = 0$ and consider only the lowest Γ_3 state. $\partial F / \partial \epsilon_3 = 0$ gives the order parameter and is shown in Fig. 15. One clearly sees the salient features proposed above: A discontinuity, increasing in temperature with increasing field and at the same time diminishing in size till it disappears completely above a certain field. Also note that the order parameter is always non-zero for finite temperatures and nonzero fields. While the parameters, taken for the plot in Fig. 15 are not yet optimized to compare quantitatively with T_a^* in Fig. 14, they certainly give the essential features. If this is the correct explanation for our results in Figs. 11–14, it would be the first time one has observed an increase in the structural transition temperature due to an external magnetic field.

V. SUMMARY

We have shown experimental results of specific heat, magnetic susceptibility, electrical resistance,

and elastic constants for TmCd and tried to interpret them. From the electrical resistance results and a point-charge calculation we arrived at a crystal-field-level scheme, which accounts for many of our results even in a quantitative way.

There is no doubt that the lowest-crystal-field level is an orbitally degenerate, nonmagnetic state (Γ_3) which gives rise to the cooperative Jahn-Teller transition at 3.16 K. Thermal, electrical, and elastic measurements and the near absence of susceptibility anomalies support this fact. From the elastic $c_{11} - c_{12}$ mode behavior, we concluded that a substantial part of the quadrupole-quadrupole interaction, driving this transition is of different nature than macroscopic strain coupling. The exact nature of this quadrupole-quadrupole interaction is not known to us. It should be pointed out that for the CsCl structure the possibility of optical-phonon coupling can be ruled out.³¹ The form of the specific-heat curve does not show a molecular-field-type behavior as seen for example in TbVO₄,³² in agreement with our analysis that part of the effective quadrupole-quadrupole interaction is of the short-range type.

Our determination of the higher-lying crystal-field levels is only approximate, as pointed out before. Because of the Cd, neutron scattering experiments are unable to get this information and because of the good metallic-conductivity, optical measurements are also difficult.

Probably the most interesting feature of our results is the apparent increase of the structural transition temperature T_a in a high magnetic field, as implied by electrical resistance and elastic constants measurements. We have given a simple tentative explanation of this fact, by showing that the first-order change of the order parameter at T_a , while decreasing in size in a magnetic field also shifts to higher temperatures. It would of course be of considerable interest to have other information on this effect. The most direct experiment would be a lattice constant determination of the structural change in the presence of a magnetic field.

ACKNOWLEDGMENTS

We thank L. D. Longinotti for growing the single crystal of TmCd and S. Darack for helping with measurements. An informative discussion with Professor P. M. Levy is gratefully acknowledged.

¹Supported in part by the National Science Foundation.

²J. D. Dunitz and L. E. Orgel, *J. Phys. Chem. Solids* **3**, 20 (1957).

³See, for example, R. J. Elliott, R. T. Harley, W. Hayes, and S. R. P. Smith, *Proc. R. Soc. A* **328**, 217 (1972).

⁴F. Lévy, *Phys. Kondens. Mater.* **10**, 85 (1969).

⁵E. Bucher, R. J. Birgenau, J. P. Maita, G. P. Felcher, and T. O. Brun, *Phys. Rev. Lett.* **28**, 746 (1972).

⁶O. G. Brandt and C. T. Walker, *Phys. Rev. Lett.* **18**, 11 (1967).

⁷Y. Kino, B. Lüthi, and M. E. Mullen, *J. Phys. Soc. Jap.* **33**, 687 (1972); *Solid State Commun.* **12**, 275 (1973).

- ⁷Unpublished results from our laboratory.
- ⁸R. L. Melcher and B. A. Scott, *Phys. Rev. Lett.* **28**, 607 (1972).
- ⁹J. R. Sandercock, S. B. Palmer, R. J. Elliott, W. Hayes, S. R. P. Smith, and A. P. Young, *J. Phys. C* **5**, 3126 (1972).
- ¹⁰R. L. Melcher (private communication).
- ¹¹G. Gorodetsky, Y. Kino, and B. Lüthi, in *International Conference on Phonon Scattering in Solids*, Paris, 1972, p. 333 (unpublished).
- ¹²T. J. Moran, R. L. Thomas, P. M. Levy and H. A. Chen, *Phys. Rev. B* **7**, 3238 (1973).
- ¹³A. Iandelli and A. Palenzola, *J. Less-Common Met.* **9**, 1 (1965).
- ¹⁴R. M. Bozorth, H. J. Williams, and J. E. Walsh, *Phys. Rev.* **103**, 572 (1956).
- ¹⁵F. J. Morin and J. P. Maita, *Phys. Rev.* **129**, 1 (1963).
- ¹⁶T. J. Moran and B. Lüthi, *Phys. Rev.* **187**, 710 (1969).
- ¹⁷K. R. Lea, M. J. M. Leask, and W. P. Wolf, *J. Phys. Chem. Solids* **23**, 1381 (1962).
- ¹⁸M. Kataoka and J. Kanamori, *J. Phys. Soc. Jap.* **32**, 113 (1972).
- ¹⁹E. Pytte and K. W. H. Stevens, *Phys. Rev. Lett.* **27**, 862 (1971).
- ²⁰See, for example, M. T. Hutchings, in *Solid State Physics*, edited by F. Seitz and D. Turnbull (Academic, New York, 1964), Vol. 16, p. 227.
- ²¹P. M. Levy (unpublished).
- ²²B. Lüthi, M. E. Mullen, K. Andres, and E. Bucher, *Bull. Am. Phys. Soc.* **18**, 34 (1973).
- ²³K. C. Turberfield, L. Passell, R. J. Birgenau, and E. Bucher, *J. Appl. Phys.* **42**, 1746 (1971).
- ²⁴K. Andres (unpublished data).
- ²⁵D. P. Schumacher and C. A. Hollingsworth, *J. Phys. Chem.* **70**, 749 (1966).
- ²⁶B. R. Cooper, *Phys. Lett.* **22**, 24 (1966).
- ²⁷See, for example, C. W. Garland, in *Physical Acoustics*, edited by W. P. Mason (Academic, New York, 1970), Vol. VII; B. Lüthi, T. J. Moran and R. J. Pollina, *J. Phys. Chem. Solids* **31**, 1741 (1970); G. Gorodetsky, B. Lüthi, and T. J. Moran, *Int. J. Magn.* **1**, 295 (1971).
- ²⁸K. A. Gehring, A. P. Malozemoff, W. Staude, and R. M. Tyte, *Solid State Commun.* **9**, 511 (1971).
- ²⁹R. P. Hudson and B. W. Mangum, *Phys. Lett. A* **36**, 157 (1971); G. Gorodetsky, B. Lüthi, and B. M. Wanklyn, *Solid State Commun.* **9**, 2157 (1971).
- ³⁰B. W. Mangum, J. N. Lee, and H. W. Moos, *Phys. Rev. Lett.* **27**, 1517 (1971); R. T. Harley, W. Hayes, and S. P. R. Smith, *J. Phys. C* **5**, 1501 (1972).
- ³¹P. M. Levy (private communication).
- ³²M. R. Wells and R. D. Worswick, *Phys. Lett. A* **42**, 269 (1972).